Trace arsenic quantification by hydride generation-flame atomic absorption spectrometry using durian husk-derived nanocellulose as a solid-phase extraction biosorbent

Tuan-Hoang Dinh[1], Sy-Chung Giang[1], Thi-Kieu-Anh Tran[2,3], Trung Dang-Bao[2,3,*]

[1]Faculty of Technology, University of Phan Thiet, Phan Thiet City, Binh Thuan Province, Vietnam

[2]Faculty of Chemical Engineering, Ho Chi Minh City University of Technology (HCMUT), 268 Ly Thuong Kiet Street, District 10, Ho Chi Minh City, Vietnam

[3]Vietnam National University Ho Chi Minh City, Linh Trung Ward, Thu Duc City, Ho Chi Minh City, Vietnam

[*]Corresponding author:

E-mail: dbtrung@hcmut.edu.vn

GRAPHICAL ABSTRACT

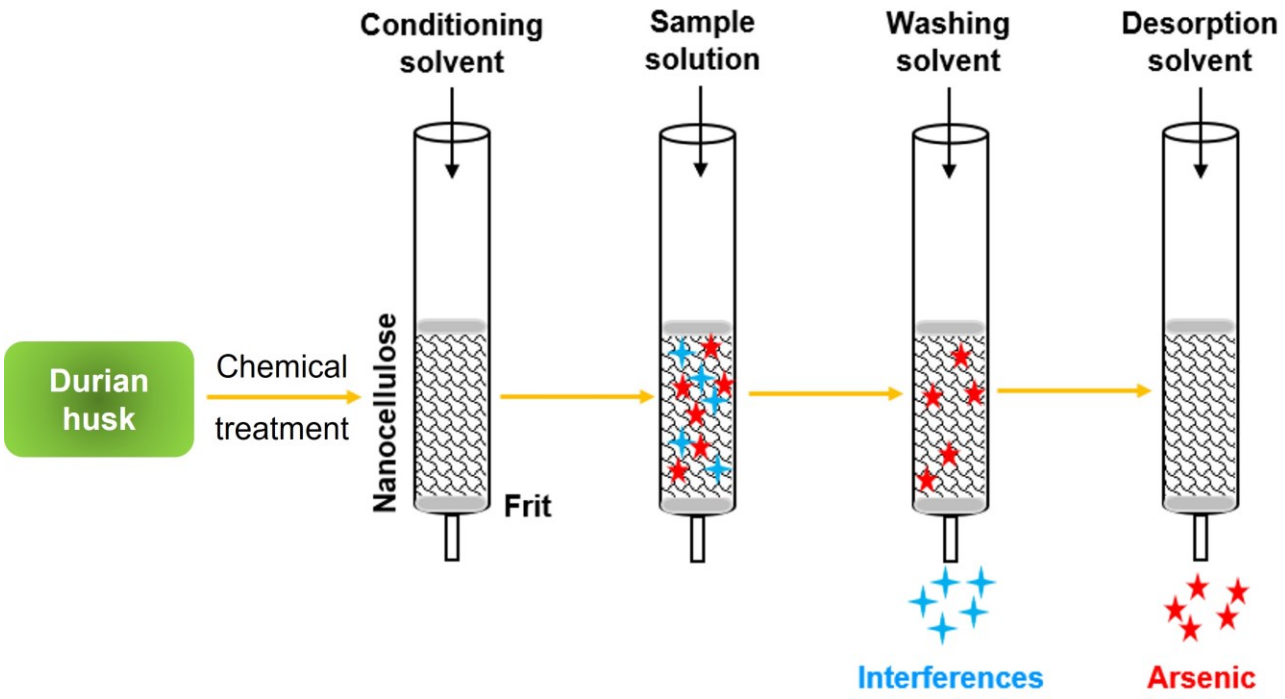

ABSTRACT

In the present study, nanocellulose was successfully extracted from durian husk via chemical treatment and then characterized by several analytical techniques, involving X-ray diffraction (XRD), Fourier-transform infrared spectroscopy (FT-IR), energy-dispersive X-ray spectroscopy (EDX) and

transmission electron microscopy (TEM). Nanocellulose was obtained with a crystallinity index of 77% and in the form of cellulose nanofibrils (30 nm in width and micrometers in length). Using nanocellulose as a biosorbent in solid-phase extraction technique, the inorganic arsenic ions were eluted using 0.1 M HNO_3 and its content in the eluate solution was quantified by hydride generation-flame atomic absorption spectrometry (HG-FAAS), in which the recovery of arsenic ions using nanocellulose were assessed via contact time, pH and dosage of sorbent, reaching the equilibrium after 30 minutes. With the limit of detection (LOD) of 0.41 ng mL^{-1}, the limit of quantification (LOQ) of 1.38 ng mL^{-1} and the relative standard deviation of repeatability (%RSD) of 3.44% (with ten replicates) for arsenic determination, the present method was practiced with the trace inorganic arsenic quantification in real samples (fish sauce with various protein levels) with reliable spike recoveries.

Keywords: atomic absorption spectrometry, arsenic, trace analysis, nanocellulose, solid-phase extraction

1. Introduction

The trace analysis of heavy metals in aqueous solutions generally requires their extraction and preconcentration, aiming at improving the sensitivity and accuracy of analytical procedures. In comparison with chemical precipitation or liquid-liquid extraction using large amounts of toxic solvents, complicated multi-steps and ineffective sample cleanup, solid-phase extraction (SPE) has gained great interest in the field of trace metal analysis (Abdolmohammad-Zadeh et al., 2020; Hanhauser et al., 2020; Khan et al., 2020; Manousi et al., 2021; Mirabi et al., 2015). The predominant features of the SPE technique involve high selectivity and preconcentration efficiency, minimal use of solvents, easy operation and automation, cost-effectiveness and time-saving. The performance of SPE column is highly dependent on the adsorbent acting as the stationary phase. Some traditional adsorbents were previously reported, such as carbon-based materials (Khaleel et al., 2018; Soylak and Maulana, 2021; Wang et al., 2020), resins (Li et al., 2014; Yang et al, 2021) and modified silica (Ghaedi et al., 2012; Rajabi et al., 2015). In order to improve the selectivity of metal adsorption, solid

materials could be functionalized with Lewis bases as metal anchors (Castro et al., 2011). However, such functionalization was generally performed in multi-step procedures, using highly purified reagents and toxic organic solvents, leading to the development of alternative natural adsorbents from the sustainability concepts.

Lignocellulosic biomass possessing carboxylate and phenolate groups in nature permits anchoring metal ions, facilitating its ability in metal adsorption (Castro et al., 2011; Thach-Nguyen and Dang-Bao, 2022). As an abundant and available resource, nanocellulose produced from agricultural by-products has recently attracted much attention in diverse applications thanks to high crystallinity, good mechanical properties, and flexible chemical reactivity based on hydroxyl groups, etc. (Li et al., 2021; Trache et al., 2020). For instance, the contents of durian husk are similar to wood fibers, consisting of ~60% cellulose (Lee et al., 2018; Lubis et al., 2018). As one of the most important fruit crops of Southeast Asia and an annual increase in production volume, durian husk has become a good candidate to produce nanocellulose for diverse applications. Taking into account of natural hydroxyl groups or modified groups on the surface of nanocellulose, such a nanomaterial promises a good solid phase for the SPE technique for the uptake of metal ions from aqueous solutions.

In aqueous solutions, inorganic arsenic species have been admitted as the most poisonous risk, being harmful to human health and classified as carcinogenic substances (according to the International Agency for Research on Cancer). Efforts in establishing the limits of arsenic in real samples have been studied, for example, the World Health Organization reported that arsenic is one of ten substances related to public health and the maximum limit of 10 ppb arsenic in drinking water. Frequently, the quantitation of arsenic species could be carried out via coupled techniques, involving chromatographic and spectroscopic methods (Bhat et al., 2023; Frisbie and Mitchell, 2022). However, the existing methods for the arsenic quantification require complicated multi-steps sampling and time consuming; in particular, in some cases, inorganic arsenic should be rapidly quantified instead of organic species. In the present work, nanocellulose was extracted from durian husk via chemical treatment and then applied to recover inorganic arsenic from an aqueous solution prior to trace arsenic

quantification by hydride generation-flame atomic absorption spectrometry (HG-FAAS). The analytical procedure was practically applied to quantify inorganic arsenic in fish sauce samples.

2. Materials and methods

2.1. Chemicals and reagents

As analytical reagent grades, all the chemicals were directly used without further purification, involving nitric acid (63%, Xilong Scientific), sulfuric acid (98%, Xilong Scientific), sodium hydroxide (99%, Xilong Scientific) and arsenic standard solution (1000 ppm As, Merck). Ultrapure water was prepared in the laboratory.

2.2. Extraction and characterization of nanocellulose from durian husk

Durian husk was collected from a local market in Binh Thuan province (Vietnam). The extraction procedure of nanocellulose from durian husk was inherited from our previous report with some minor modifications (Thach-Nguyen et al., 2022). After washing with distilled water, durian husk was ground and dried at 100 °C overnight. In order to remove hemicellulose and lignin, 100.0 g raw material was added to 200.0 mL of 2.0 M HNO_3 solution and the blend was stirred at 80 °C for 2 hours. After finishing the process, the solid was filtered and washed with distilled water. The acid treatment procedure was repeated 3 times and successively treated with 200.0 mL of 5% NaOH solution at 80 °C for 2 hours. After being centrifuged at 8,000 rpm and washed until pH 7, the bleaching was followed using 5% H_2O_2 solution. Washed product (5.0 g) was finally acid hydrolyzed using 100.0 mL of 64% H_2SO_4 solution at 80 °C for 8 hours, yielding nanocellulose after being centrifuged at 10,000 rpm and washed until pH 7.

The characteristics of as-prepared nanocellulose from durian husk were examined on D2 Bruker powder X-ray diffractometer (XRD) with a Cu-Kα radiation (λ =1.5406 Å) and 2θ of 5−80°, Tensor 27 Bruker Fourier-transform infrared (FT-IR) spectrometer in the range of 4000–400 cm^{-1}, JEOL JST-IT 200 energy-dispersive X-ray spectrometer (EDX), and JEOL JEM 1400 transmission electron microscope (TEM).

2.3. Recovery of inorganic arsenic from an aqueous solution using solid-phase extraction nanocellulose

Typically, 20.0 mL of arsenic (V) ion solution (100.0 ng mL^{-1}) was adjusted to pH 4 using phosphoric acid buffer solution and then added to a syringe containing 0.5 g nanocellulose. After 30 minutes, the syringe was first eluted using methanol (3 × 5.0 mL), and the inorganic arsenic ions were then eluted from the adsorbent using 0.1 M HNO_3 solution (3 × 5.0 mL). The eluate solution was made up to 25.0 mL using 0.1 M HNO_3 solution. A quantitative reduction of As(V) toward As(III) in 10.0 mL of the above solution was achieved by adding 2.0 mL of 5% KI and 5% ascorbic acid solution, 4.0 mL of concentrated HCl solution at room temperature for 1 hour. After making up to 50.0 mL, the arsenic content was quantified by hydride generation-flame atomic absorption spectrometry (HG-FAAS, AA-7000 Shimadzu). An arsenic hollow cathode lamp was applied as an irradiation source at the wavelength of 193.7 nm for arsenic, operated at 10.0 mA with a slit width of 1.3 nm. An air-acetylene flame was utilized with their respective flow rates of 15.0 and 1.2 L min^{-1}.

The arsenic extraction efficiency from nanocellulose was examined via adsorption parameters, involving contact time (10–60 minutes), pH (2–10) and dosage of adsorbent (0.1–1.0 g). The adsorption behavior was also evaluated using the Langmuir and the Freundlich isotherms as equation (1) and (2).

$$\frac{C_e}{q_e} = \frac{1}{K_L q_m} + \frac{C_e}{q_m} \qquad (1)$$

$$\lg q_e = \lg K_F + \frac{1}{n}\lg C_e \qquad (2)$$

Where C_e represents equilibrium concentration (ng mL^{-1}); q_e and q_m represent equilibrium and maximum adsorption capacities (µg g^{-1}); K_L, K_F and n represent Langmuir, Freundlich and heterogeneity coefficients.

2.4. Determination of inorganic arsenic from a fish sauce using solid-phase extraction nanocellulose

The real samples (fish sauce collected from a local market) were treated following the above procedure at the optimal conditions. In more detail, 20.0 mL of sample solution was adjusted to pH

4 using phosphoric acid buffer solution and then added to a syringe containing 0.5 g nanocellulose. After 30 minutes, the syringe was first eluted using methanol (3 × 5.0 mL) and the inorganic arsenic ions were then eluted from adsorbent using 0.1 M HNO_3 solution (3 × 5.0 mL). The eluate solution was made up to 25.0 mL using 0.1 M HNO_3 solution. A quantitative reduction toward As(III) in 10.0 mL of the above solution was achieved by adding 2.0 mL of 5% KI and 5% ascorbic acid solution, 4.0 mL of concentrated HCl solution at room temperature for 1 hour. Finally, the resulting solution was made up to 50.0 mL. The standard addition method was addressed using spiked real samples and the calibration curve was constructed in a range of 0.4–12.0 ng mL^{-1}.

For a comparative study, the determination of inorganic arsenic in a fish sauce sample was also carried out according to the internal validation method that established from the protocol of Calle et al. (Calle et al., 2017) with some minor modifications. Briefly, 2.0 mL of sample solution and 4.0 mL of distilled water were well-mixed for 5 minutes, and then 18.0 mL of concentrated HCl (37−38%) was added to the above solution, agitated for 15 minutes. Further hydrolysis occurred by resting for 12−15 hours. Next, 2.0 mL of HBr (48%, w/v) and 1.0 mL of hydrazine (15 mg/mL) were added to the hydrolyzed solution and then shaken for 30 seconds. Add 10.0 mL of $CHCl_3$ and shake 5 minutes. After centrifuging for 5 minutes, the chloroform phase was extracted from the acid phase (2 times), and the collected chloroform phase was centrifuged for 5 minutes to remove all acid phase residues. The chloroform phase was filtered using a PTFE membrane (0.45 μm). Next, 5.0 mL of 2% HNO_3 solution was added, shaken for 5 minutes and rested for 1 minute. The acid phase (upper phase) was collected and then mineralized by heating until transparent. After cooling to room temperature, the obtained solution was made up to 50.0 mL using distilled water. A quantitative reduction toward As(III) in 10.0 mL of the above solution was achieved by adding 2.0 mL of 5% KI and 5% ascorbic acid solution, 4.0 mL of concentrated HCl solution at room temperature for 1 hour. After making up to 50.0 mL, the arsenic content was quantified by HG-FAAS.

2.5. Method validation

The validation of the analytical method was obeyed according to the Association of Official Analytical Chemists (AOAC) (AOAC, 2007) and the International Conference on Harmonisation (ICH Q2(R1)) (ICH, 2005) guidelines, involving linearity, limits of detection (LOD) and quantification (LOQ), precision (repeatability relative standard deviation on a single day, %RSD), and accuracy (recovery). The linear regression was evaluated on the calibration curve by plotting the absorbances of various arsenic concentrations (0.4–12.0 ng mL^{-1}) and the coefficient of determination (r^2). The values of %RSD, LOD and LOQ were respectively determined from the blank samples spiked with known arsenic concentrations for ten replicates (n = 10). The standard addition method was addressed using spiked real samples (fish sauce samples with various protein levels), permitting determining the recovery from ten replicates.

3. Results and Discussion

3.1. Characteristics of durian husk-derived nanocellulose

Unlike cellulose possessing both crystalline and amorphous regions, hemicellulose and lignin are amorphous that can be efficiently removed by chemical reagents (Andersson et al., 2003; Thach-Nguyen et al., 2022). Therefore, the isolation efficiency of cellulose from the plant cell walls was evaluated via crystallinity index (I_C) from XRD data (Li et al., 2021; Thach-Nguyen et al., 2022).

$$I_C\ (\%) = \frac{I_{22.6} - I_{18.8}}{I_{22.6}} \times 100$$

Where $I_{22.6}$ and $I_{18.8}$ are the diffraction intensity recorded at 2θ of 22.6° (crystalline phase) and 18.8° (amorphous phase), respectively.

The crystalline structure of as-prepared cellulose was confirmed via powder XRD method (Figure 1), representing the diffraction peaks at 15.6°, 22.6° and 34.7° attributed to (110), (200) and (004) planes, respectively (Li et al., 2021; Thach-Nguyen et al., 2022). The crystallinity index of 77% was estimated from the XRD data, evidencing the efficient isolation of crystalline cellulose from amorphous regions (such as hemicellulose and lignin). This crystallinity index was established in the range of 54–88%, in agreement with previously reported nanocelluloses (involving cellulose

nanocrystals and cellulose nanofibrils) (Thach-Nguyen et al., 2022; Trache et al., 2020). According to the Debye-Scherrer equation estimated at the crystalline plane of (200), the average crystallite size of cellulose was 4.6 nm, very close to the previous report (Gong et al., 2017).

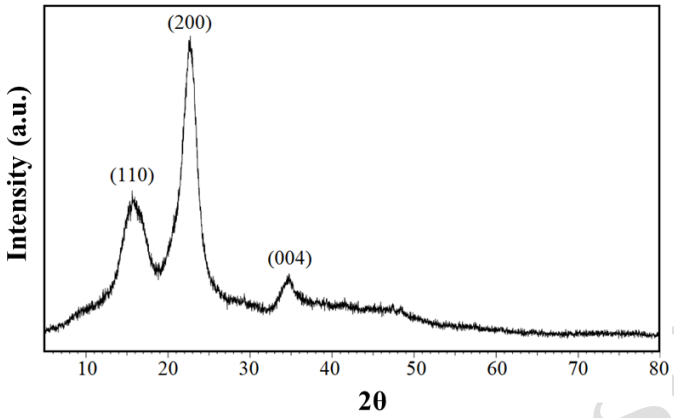

Figure 1. XRD pattern of durian husk-derived nanocellulose

The presence of cellulose as a major component was observed via its vibrational bands of functional groups from FT-IR spectrum (Figure 2). Typically, the absorption bands at 3409 cm^{-1} and 1640 cm^{-1} were assigned to O–H stretching, evidencing the hydrophilic property of cellulose fibers (Raza et al., 2022; Thach-Nguyen et al., 2022; Wang et al., 2019). The bands at 2900 cm^{-1} (C–H stretching) and 1431–1318 cm^{-1} (C–H stretching and $–CH_2$ vibration) were also assigned to crystalline cellulose (Li et al., 2021). The band at 1162 cm^{-1} was attributed to the C–O–C glycosidic ether; and the bands at 1162–1033 cm^{-1} were associated with C–O / C–O–C stretching (Li et al., 2021). The band at 898 cm^{-1} corresponded to C–O–C vibration and C–H rocking vibration (Li et al., 2021; Raza et al., 2022; Thach-Nguyen et al., 2022). In principle, the isolation of nanocellulose could occur based on the chemical attacks to C–O / C–O–C linkages; therefore, the bands at 1162–1033 cm^{-1} and 898 cm^{-1} were typical to both amorphous and crystalline regions of cellulose (Li et al., 2021; Thach-Nguyen et al., 2022). In particular, the absence of the absorption bands at 1730 cm^{-1} (uronic ester and acetyl groups coming from hemicellulose, carboxylic groups of ferulic and p-coumaric acids coming from lignin) and 1240 cm^{-1} (aryl group from lignin) affirmed the efficient isolation of cellulose fibers from hemicellulose and lignin (Raza et al., 2022; Thach-Nguyen et al., 2022).

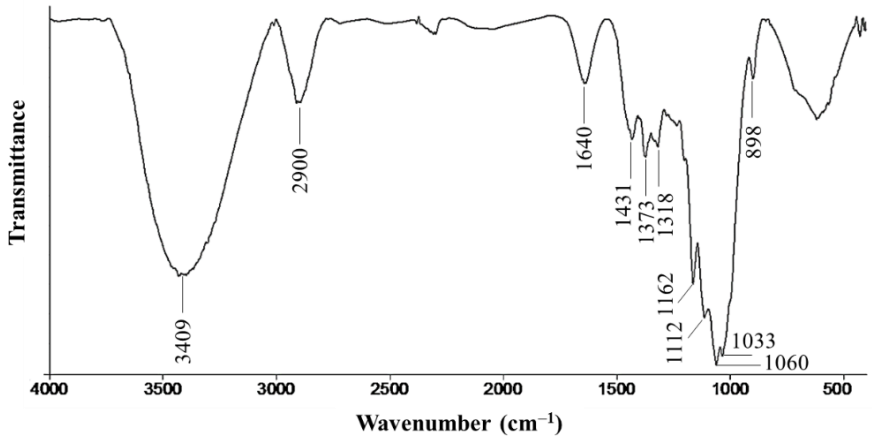

Figure 2. FT-IR spectrum of durian husk-derived nanocellulose

The elemental composition of the isolated solid surface was also analyzed via EDX technique (Figure 3), indicating the molar ratio of carbon and oxygen regarding the empirical formula of cellulose ($C_6H_{10}O_5$). The major presence of cellulose in the isolated product was agreeable to the fact that cellulose was successfully isolated from lignin and hemicellulose (Thach Nguyen et al., 2022).

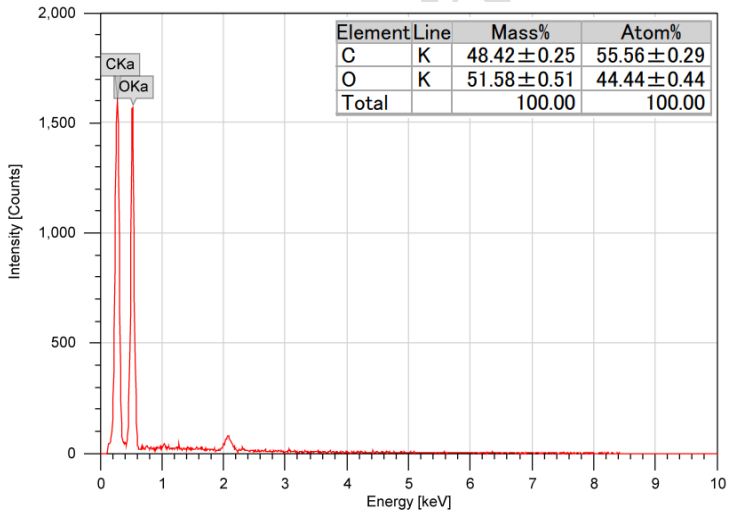

Figure 3. EDX spectrum of durian husk-derived nanocellulose

TEM image showed the formation of cellulose nanofibrils with 30 nm in width and micrometers in length (Figure 4). Together with the crystallinity index in the range of 54–88% (Thach-Nguyen et al., 2022; Trache et al., 2020), it can be concluded that nanocellulose was obtained with the crystallinity index of 77% and the morphology in the form of cellulose nanofibrils (CNFs) (Noremylia et al., 2022; Trache et al., 2020). In principle, cellulose has both crystalline and amorphous regions (Andersson et al., 2003; Thach-Nguyen et al., 2022), in which chemical reagents can efficiently attack amorphous

regions and thus glycosidic linkages can be easily broken, resulting in smaller fragments. Therefore, their size and shape are rationally dependent on the nature of cellulosic sources and the treatment conditions (Noremylia et al., 2022; Thach-Nguyen et al., 2022; Trache et al., 2020).

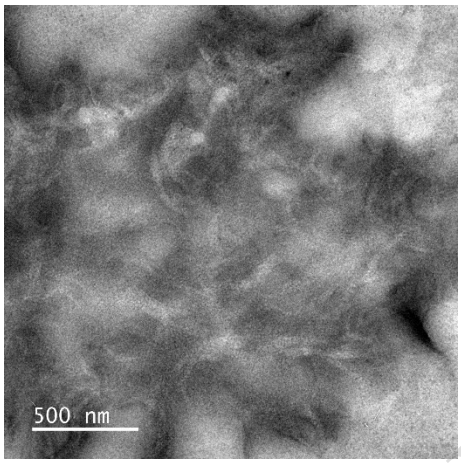

Figure 4. TEM image of durian husk-derived nanocellulose

3.2. Evaluation of extraction efficiency of inorganic arsenic from an aqueous solution using nanocellulose biosorbent

The arsenic extraction efficiency from nanocellulose was assessed via adsorption parameters involving contact time, pH and dosage of nanocellulose, with the initial arsenic concentration of 100.0 ng mL^{-1} (Figure 5). The extraction recovery showed a proportion of arsenic ions retained on nanocellulose, which was quantified in the eluate solution using 0.1 M HNO_3 solution as a desorption reagent by HG-FAAS. The equilibrium was reached after 30 minutes, and the highest recovery of arsenic ions desorbed from nanocellulose was obtained at pH 4, using 0.5 g nanocellulose. Anchoring arsenic ions onto the surface of nanocellulose could be attributed to the electrostatic attraction with the hydroxyl groups and sulfate groups generated during sulfuric acid hydrolysis (Thach-Nguyen and Dang-Bao, 2022; Thach-Nguyen et al., 2022).

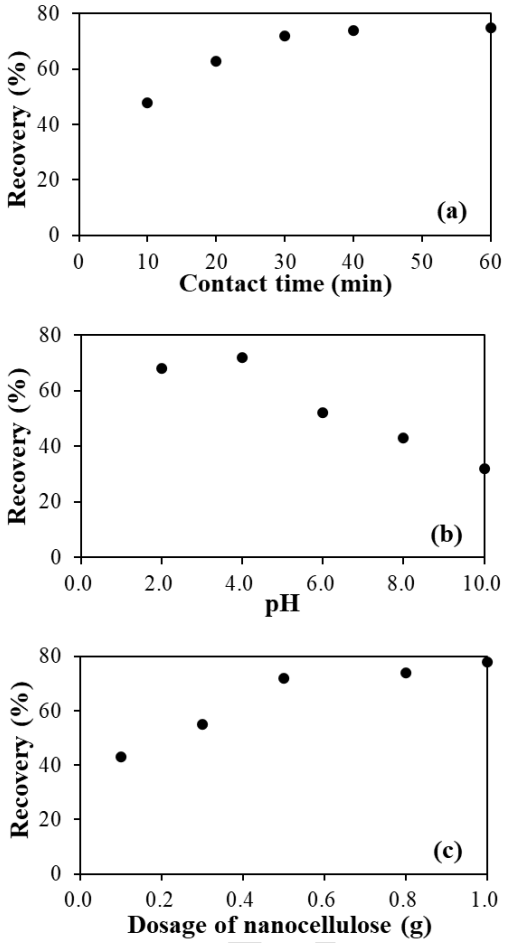

Figure 5. Effects of contact time (a), pH (b), and dosage of nanocellulose (c) on the arsenic sorption

At room temperature and pH 4, the equilibrium arsenic adsorption capacity of nanocellulose was raised with an increase in initial arsenic concentration from 25.0 to 200.0 ng mL^{-1}, using 0.1 g nanocellulose. Such adsorption of arsenic in an aqueous solution on nanocellulose obeyed both the Langmuir (R^2 = 0.9954) and the Freundlich isotherms (R^2 = 0.9957) (Figure 6) (Huang et al., 2020; Dang-Bao et al., 2021). Other adsorption parameters from both isotherm models were summarized in Table 1. According to the Langmuir isotherm, the monolayer adsorption was estimated with a maximum adsorption capacity of 26.46 µg g^{-1}. The predominance of chemisorption can be derived from ion exchange, surface coordination, or electrostatic forces between arsenic cations and electron-rich oxygen-containing functional groups (hydroxyl, carboxylic) on the nanocellulose's surface (Dang-Bao et al., 2023).

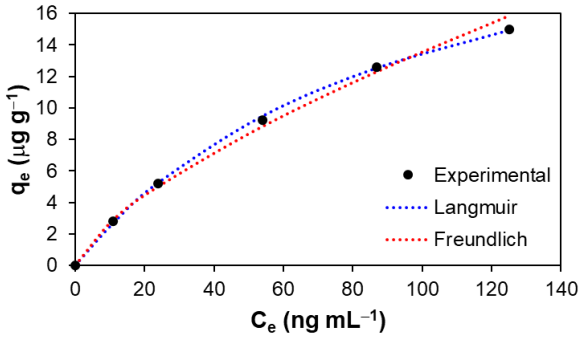

Figure 6. The arsenic adsorption on nanocellulose simulated according to the Langmuir and the Freundlich isotherms

Table 1. Langmuir and Freundlich isotherms for arsenic adsorption on nanocellulose

Langmuir			Freundlich		
q_m (µg g^{-1})	K_L	R^2	n	K_F	R^2
26.46	0.0103	0.9954	1.43	0.5483	0.9957

3.3. Quantification of inorganic arsenic in real samples using solid-phase extraction technique

Using the solid-phase extraction technique to extract inorganic arsenic in a real sample of fish sauce, the inorganic arsenic concentration in the eluate solution was then quantified by HG-FAAS. The analytical method was well-performed with a linearity range of 0.4–12.0 ng mL^{-1} and a reasonable determination coefficient of 0.9998. The spiked samples were analyzed with ten replicates, showing the limit of detection (LOD) of 0.41 ng mL^{-1}, the limit of quantification (LOQ) of 1.38 ng mL^{-1}, the repeatability relative standard deviation (%RSD) of 3.44% (Table 2). The effect of interfering ions on the recovery of arsenic spiked at 50 ng mL^{-1} was briefed in Table 3, evidencing minimal errors in recovering arsenic compared to the certified sample. The real samples of fish sauce with different protein levels (20°N and 40°N) were quantitatively analyzed by both the proposed method and the internal validation method, showing the inorganic arsenic contents in the eluate solution with values below the limit of detection. The spiked samples indicated the recovery and the repeatability in the acceptable ranges, according to the AOAC and the ICH guidelines (Table 4). In comparison with the internal validation method using a large amount of toxic organic solvents with complicated multi-

steps, the present analytical method based on the solid-phase extraction technique was still reliable in the trace quantification of inorganic arsenic in fish sauce, with some advantages such as high accuracy, easy operation, cost-effective and time-saving. Furthermore, biomass-derived nanocellulose proposed the potential biosorbent in the solid-phase extraction technique with good retention.

Table 2. Parameters for the proposed analytical procedure

Parameter	
Linearity range (ng mL^{-1})	0.4–12.0
Linear equation	y = 0.0106x – 0.0014
Coefficient of determination (r^2)	0.9998
Limit of detection (LOD, ng mL^{-1}) (n = 10)	0.41
Limit of quantification (LOQ, ng mL^{-1}) (n = 10)	1.38
Repeatability (%RSD) (n = 10)	3.44

Table 3. Effect of interfering ions on the recovery of arsenic spiked at 50 ng mL^{-1}

Interfering ions	Added as	Concentration (mg mL^{-1})	Recovery (%)
Na^+	NaCl	80	92.4
Ca^{2+}	$CaCl_2$	70	92.4
NH_4^+	NH_4Cl	20	92.2
NH_4^+	NH_4Cl	40	91.9
Fe^{3+}	$FeCl_3$	0.04	91.4
Fe^{2+}	$FeCl_2$	0.04	91.7

Table 4. Quantification of inorganic arsenic in real and spiked samples

Sample	Arsenic spiked (ng mL^{-1})	Proposed method		Internal validation method	
		Arsenic detected (ng mL^{-1})	Recovery (%)	Arsenic detected (ng mL^{-1})	Recovery (%)
Fish sauce (20°N)[a]	-	BLOD[c]	-	BLOD[c]	-
	50[b]	4.61 (0.15)[d]	92.3	4.92 (0.13)[d]	98.4
Fish sauce (40°N)[a]	-	BLOD[c]	-	BLOD[c]	-
	50[b]	4.17 (0.12)[d]	83.3	4.60 (0.18)[d]	92.0

[a] Protein levels

[b] Ten-fold dilution before quantification
[c] Below the limit of detection
[d] Standard deviation (SD) of ten replicates

4. Conclusions

In the present work, durian husk-derived nanocellulose was utilized as the biosorbent in the solid-phase extraction technique, showing good retention in the determination of inorganic arsenic in fish sauce samples. The quantification of arsenic concentration in the eluate solution followed by HG-FAAS was reliable with the relative standard deviation of repeatability and spike recovery, adapting in the acceptable ranges authorized by the AOAC and the ICH. The proposed method showed relatively low limits of detection and quantification, permitting widening the applications in trace metal analysis in an aqueous solution. The inorganic arsenic concentrations analyzed from real samples showed values below the limit of detection.

Acknowledgements

We acknowledge University of Phan Thiet and Ho Chi Minh City University of Technology (HCMUT), VNU-HCM for supporting this study.

References

Abdolmohammad-Zadeh H., Ayazi Z. and Hosseinzadeh S. (2020), *Microchemical Journal*, **153**, 104268.

Andersson S., Serimaa R., Paakkari T., Saranpää P. and Pesonen E. (2003), *Journal of Wood Science*, **49**, 531–537.

AOAC International: How to meet ISO 17025 requirements for method verification, USA (2007).

Bhat A., Hara T.O., Tian F. and Singh B. (2023), *Environmental Science: Advances*, **2**, 171–195.

Calle M.B., Devesa V., Fiamegos Y. and Vélez D. (2017), *Journal of Visualized Experiments*, **127**, e55953.

Castro R.S.D., Caetano L., Ferreira G., Padilha P.M., Saeki M.J., Zara L.F., Martines M.A.U. and Castro G.R. (2011), *Industrial & Engineering Chemistry Research*, **50**, 3446–3451.

Dang-Bao T., Lam H.H. and Dang T.H.L. (2021), *IOP Conference Series: Earth and Environmental Science*, **947**, 012026.

Dang-Bao T., Nguyen T.M.C., Hoang G.H., Lam H.H., Phan H.P., Tran T.K.A. (2023), *Polymers*, **15**, 2562.

Frisbie S.H. and Mitchell E.J. (2022), *PLoS ONE*, **17**, e0263505.

Ghaedi M., Rezakhani M., Khodadoust S., Niknam K. and Soylak M. (2012), *The Scientific World Journal*, **2012**, 764195.

Gong J., Li J., Xu J., Xiang Z. and Mo L. (2017), *RSC Advances*, **7**, 33486–33493.

Hanhauser E., Bono Jr.M.S., Vaishnav C., Hart A.J. and Karnik R. (2020), *Environmental Science & Technology*, **54**, 2646–2657.

Huang H., Wang Y., Zhang Y., Niu Z. and Li X. (2020), *Open Chemistry*, **18**, 97−107.

Khaleel A.I., Raoof A. and Tuzen M. (2018), *Atomic Spectroscopy*, **39**, 235–241.

Khan W.A., Arain M.B. and Soylak M. (2020), *Food and Chemical Toxicology*, **145**, 111704.

Lee M.C., Koay S.C., Chan M.Y., Pang M.M., Chou P.M. and Tsai K.Y. (2018), *MATEC Web of Conferences*, **152**, 02007.

Li H., Liu J., Zhu L., Gao X., Wei S., Guo L., Zhang S. and Liu X. (2014), *Solvent Extraction Research and Development, Japan*, **21**, 147−161.

Li M., He B., Chen Y. and Zhao L. (2021), *ACS Omega*, **6**, 25162–25169.

Lubis R., Saragih S.W., Wirjosentono B. and Eddyanto E. (2018), *AIP Conference Proceedings*, **2049**, 020069.

Manousi N., Kabir A., Furton K.G., Zachariadis G.A. and Anthemidis A. (2021), *Separations*, **8**, 100.

Mirabi A., Dalirandeh Z. and Rad A.S. (2015), *Journal of Magnetism and Magnetic Materials*, **381**, 138–144.

Noremylia M.B., Hassan M.Z. and Ismail Z. (2022), *International Journal of Biological Macromolecules*, **206**, 954–976.

Rajabi M., Barfi B., Asghari A., Najafi F. and Aran R. (2015), *Food Analytical Methods*, **8**, 815–824.

Raza M., Abu-Jdayil B., Banat F. and Al-Marzouqi A.H. (2022), *ACS Omega*, **7**, 25366–25379.

Soylak M. and Maulana R. (2021), *International Journal of Environmental Analytical Chemistry*, 1–13.

Thach-Nguyen R. and Dang-Bao T. (2022), *IOP Conference Series: Materials Science and Engineering*, **1258**, 012014.

Thach-Nguyen R., Lam H.H., Phan H.P. and Dang-Bao T. (2022), *RSC Advances*, **12**, 35436–35444.

Trache D., Tarchoun A.F., Derradji M., Hamidon T.S., Masruchin N., Brosse N. and Hussin M.H. (2020), *Frontiers in Chemistry*, **8**, 392.

Validation of Analytical Procedures: Text and Methodology Q2(R1), ICH Harmonised Tripartite Guideline (2005).

Wang J., Zhu W., Zhang T., Zhang L., Du T., Zhang W., Zhang D., Sun J., Yue T., Wang Y.C. and Wang J. (2020), *Analytica Chimica Acta*, **1100**, 57–65.

Wang Z., Yao Z., Zhou J., He M., Jiang Q., Li S., Ma Y., Liu M. and Luo S. (2019), *International Journal of Biological Macromolecules*, **129**, 1081–1089.

Yang B., Wu S.Z., Liu X.Y., Yan Z.X., Liu Y.X., Li Q.S., Yu F.S. and Wang J.L. (2021), *Rare Metals*, **40**, 2633–2644.